

Measuring Single Small Molecule Binding via Rupture Forces of a Split Aptamer

Thi-Huong Nguyen,^{1,2} Lorenz Jan Steinbock,¹ Hans-Jürgen Butt,¹ Mark Helm,^{*,2} and Rüdiger Berger^{*,1}

¹Max Planck Institute for Polymer Research, 55128 Mainz, Germany

²Institute of Pharmacy and Biochemistry, Johannes Gutenberg University Mainz, Mainz 55128, Germany

S Supporting Information

ABSTRACT: The rupture force of a split (bipartite) aptamer that forms binding pockets for adenosine monophosphate (AMP) was measured by atomic force spectroscopy. Changes in the rupture force were observed in the presence of AMP, while this effect was absent when mutant aptamers or inosine were used. Thus, changes in the rupture force were a direct consequence of specific binding of AMP to the split aptamer. The split aptamer concept allowed the detection of nonlabeled AMP and enabled us to determine the dissociation constant on a single-molecule level.

The binding of small molecules to nucleic acids is of outstanding importance in fundamental research as well as in applications in life sciences. Of particular interest are aptamers, that is, short single-stranded nucleic acids, which are typically evolved by an *in vitro* evolution protocol to bind target moieties with high affinity and specificity.^{1–3} In comparison with antibodies, aptamers show higher chemical stability.⁴ Their binding properties are easier to manipulate, and they can be raised to bind to a large variety of targets, including small organic molecules, proteins, and cells.^{1,5} In general, detection of binding to proteins and cells is facilitated by the fact that these can typically be labeled with fluorescent dyes without changing their properties. In contrast, efficient detection of small molecules suffers from significant changes of chemical properties as a consequence of target labeling and from the relative paucity of binding sites on small organic molecules.^{6,7} Congruously, a large number of aptamers have been raised against proteins,^{8,9} but comparatively few well-characterized aptamers that efficiently bind to small molecules are known. These hold great promise, for example, in biosensing^{10,11} and medical diagnostic applications,¹² as has been shown in several recent examples.^{13–17}

Atomic force spectroscopy (AFS) is a valuable tool for studying interactions on a single-molecule level,^{18–22} including aptamer–target interactions. Papamichael et al.²³ have used an aptamer-coated probe and an IgE-coated mica surface to identify specific binding areas. More quantitatively, AFS allows the determination of the rupture force of aptamer binding to proteins and cells.^{24–27} The analysis of AFS data have revealed rupture forces in the realm of several tens to hundreds of piconewtons. To date, the target molecules as well as the aptamer probes have been immobilized on the AFS tip and sample surface, respectively. However, similar to analyte-labeling approaches, this concept

suffers from the need to chemically manipulate or label the target analyte at those sites that interact with the surface. Here we have solved this problem by using a split, i.e., a bipartite aptamer. One component is immobilized on the AFS tip and the other on the sample surface. During the AFS experiment, the bipartite aptamers can transiently form defined binding pockets for the free analyte. If one is flexible in the choice of the aptamer, the approach of splitting the aptamer sequences into a bipartite structure should be widely applicable for the detection of various small molecules, such as cocaine.^{11,28} Consequently the method enables us to determine binding constants and the selectivity of molecular interactions on a single-molecule level. As an example of the bipartite concept, we outline the route to probe the binding of adenosine monophosphate (AMP, 316 Da) as small target molecules to aptamers by AFS. We used the well-known aptamer sequence 3'-ACTGGA-AGGAGG-AGATGC-GCATCT-AGGAGG-TCCAGT-5', which includes two binding pockets (underlined sequences).²⁹ For AFS, the sequence was split into two parts. The first sequence of 18 bases (oligo a, 3'-ACTGGA-AGGAGG-AGATGC-A²⁰-SH-5') was immobilized on the tip and the remaining sequence (oligo b, 5'-SH-A²⁰-TGACCT-GGAGGA-TCTACG-3') on the substrate by thiol linkers.

The spacer A²⁰ between the tip and the aptamer sequence increased the tip–sample distance at which rupture between oligo a and oligo b was expected (Figure 1). Moving the tip toward the surface resulted in partial hybridization between oligo a and oligo b (Figure 1a,b). When AMP target molecules were added to the buffer solution, two AMP molecules inserted into the binding pockets and eight additional hydrogen bonds were formed^{29–31} (Figure 1c, red lines). The rupture force could be measured during the tip–sample separation cycle (Figure 1d). We found that the rupture force (*F*) between oligo a and oligo b increased in the presence of AMP (Figure 1e) in comparison with the one measured in absence of AMP (Figure 1f).

Next, we recorded 1000 force–distance (*F*–*D*) curves and plotted the probability distributions of the rupture forces in a histogram (Figure 2). In pure buffer solution, a mean rupture force of 27.3 ± 5.4 pN was determined from a fit of the main peak in the histogram by a Gaussian distribution (Figure 2a). The error represents one standard deviation (1σ) obtained from the Gaussian fit. This rupture force is associated with the hydrogen bonds formed by 12 base pairs in the hybridized system (non-underlined sequence). The rupture force value is consistent with measurements of Strunz et al.³² under comparable conditions.

Received: October 13, 2010

Published: February 2, 2011

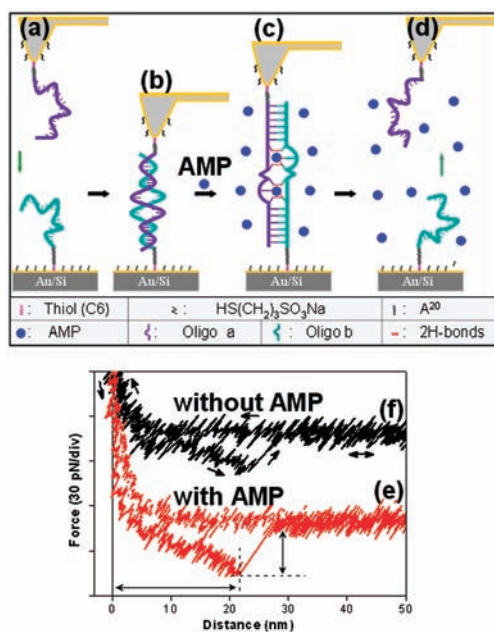


Figure 1. (a–d) Concept of measuring the rupture force of a bipartite aptamer that binds AMP. The adhesion force between the AFS tip and the sample surface was minimized by the additional immobilization of $\text{HS}(\text{CH}_2)_3\text{SO}_3\text{Na}$ (details are provided in the Supporting Information). The individual force–distance curves resulted in a rupture force of (e) ~ 39 pN in buffer containing $100 \mu\text{M}$ AMP and (f) ~ 27 pN in pure buffer. The measured mean rupture distance (L) of 17.4 ± 5.2 nm is in agreement with the calculated contour length of the designed oligos (21 nm).

Furthermore, the mean rupture force increased in proportion to the logarithm of the loading rate (Figure 4S in the Supporting Information). When the buffer solution was exchanged with one containing $100 \mu\text{M}$ AMP, an increase in the rupture force to 38.8 ± 3.9 pN was detected (Figure 2b). In addition, we observed an increase in the rupture distance from 17.4 ± 6.2 nm to 20.6 ± 3.9 nm (Figure 5S). This increase of ~ 3 nm is attributed to greater stretching of the involved oligonucleotides because of the higher rupture force values.³³ After the liquid cell was thoroughly rinsed with buffer (i.e., after the AMP molecules were washed out), the mean rupture force and rupture distance returned to the values corresponding to the initial experiment in buffer within the given experimental error (Figure 2c). We conclude that the increase in rupture force was due to binding of AMP molecules to the transiently formed binding pockets of the bipartite aptamer.

In order to determine the dissociation constant (K_D) of the AMP-binding aptamer, sets of F – D curves were recorded at concentrations ranging from 0.01 to $100 \mu\text{M}$. Subsequently, each histogram of the rupture forces was analyzed by fitting simultaneously two Gaussian distributions to the peaks corresponding to “only oligo hybridization” and to “AMP binding”, respectively (all histograms are provided in Figure 6S). With increasing concentration of AMP, the peak corresponding to “AMP binding” became more pronounced, i.e., more rupture events at higher forces were present. Simultaneously, the peak corresponding to “only oligo hybridization” was composed of fewer rupture events. More quantitatively, we analyzed the number of events associated with each Gaussian fit within each histogram. At an AMP concentration of $4 \mu\text{M}$, we determined 44 rupture events corresponding to peak 1, i.e., the peak associated with “only oligo

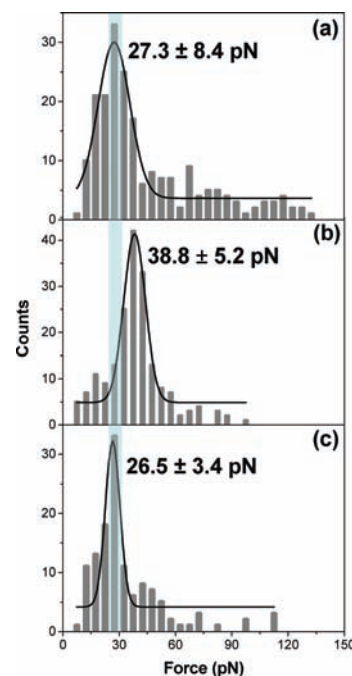


Figure 2. Histograms of the rupture force distributions, which were recorded at a speed of 400 nm/s. Typically, one-fourth of the recorded 1000 F – D curves exhibited a rupture event. (a) In the absence of AMP. (b) At $100 \mu\text{M}$ AMP. (c) After the AMP was rinsed away. The measurements summarized in the histograms (a), (b), and (c) were recorded with the same tip. Each histogram was fitted by a Gaussian distribution (black line), which defines the rupture force value and the associated error (i.e., 1σ).

hybridization” (Figure 3a, black curve). For the “AMP binding”, we determined 43 rupture events (Figure 3a, red curve). Consequently, we obtained fractions of 49 and 51% of all events corresponding to “oligo hybridization” and “AMP binding”, respectively. Both fractions were determined for each histogram recorded at a different AMP concentration, and these values are plotted in Figure 3b. For this series of measurements, we found that the fraction of the “AMP binding” events increased when the AMP concentration increased, while the one corresponding to “only oligo hybridization” decreased. Both data sets could be fitted by an exponential dependence ($y = y_0 + Ae^{-x/t}$). At a concentration of $3.7 \pm 2.5 \mu\text{M}$, we observed the crossover of both hybridization (50%) and AMP binding (50%) events. Therefore, this value was attributed to the dissociation constant of the AMP binding aptamer. This value, which was obtained on a single-molecule level, is in agreement with a measurement performed by ultrafiltration ($6 \pm 3 \mu\text{M}$).⁷

As a control experiment, we mutated the binding pocket in the aptamer by replacing the G bases at different positions (the bases shown in bold in Table 1 in the Supporting Information). For those sequences, no changes in rupture forces were observed (Figure 7S). In a second type of control experiment, we substituted AMP with inosine, a chemically similar small molecule known not to bind to the standard aptamer.²⁹ No changes in rupture forces were observed in the presence of $100 \mu\text{M}$ inosine (Figure 8S).

The measurement of the dissociation constant as well the two reference experiments demonstrate the advantage of binding the target in a transient binding pocket that is formed by the bipartite aptamer. Now that the effect of single-nucleotide mutations has

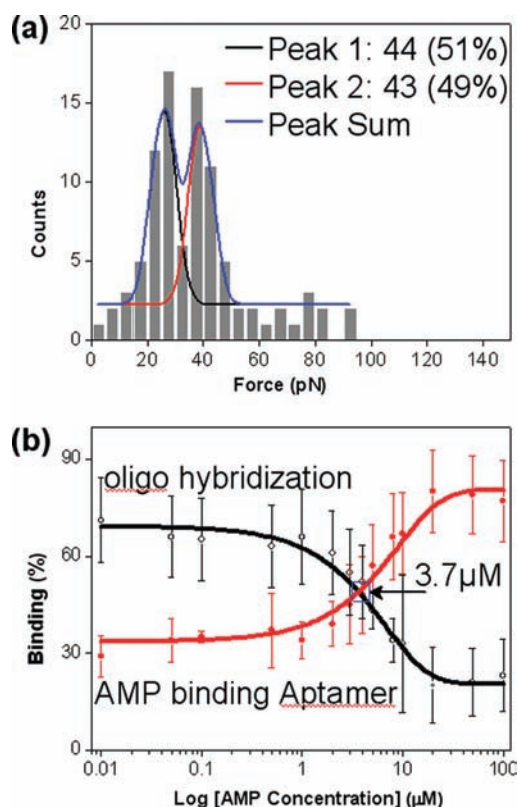


Figure 3. Determination of K_D of the AMP–aptamer system. (a) The histogram that was obtained at a concentration close to the dissociation constant. The Gaussian fits indicate hybridization of oligos only (black line), oligos with AMP (red line), and their sum (blue line). (b) Plot of the fraction of oligo hybridization and oligo–AMP binding as functions of AMP concentration. The individual histograms for the various concentrations are provided in the Supporting Information. The error bars represent 1σ from the Gaussian fits to the histograms.

been observed, it will be interesting to determine the lowest possible number of hydrogen bonds that is required for binding of small target molecules.

■ ASSOCIATED CONTENT

S Supporting Information. Experimental methods, dependence of tip velocity on rupture forces, dependence of tip velocity on rupture distances, detailed calculation of dissociation constant, rupture forces of mutant aptamers, substitution of AMP by its derivatives, dependence of rupture forces on tip velocity, and pull-off distances. This material is available free of charge via the Internet at <http://pubs.acs.org>.

■ AUTHOR INFORMATION

Corresponding Author

mhelm@uni-mainz.de; berger@mpip-mainz.mpg.de

■ ACKNOWLEDGMENT

We thank the SFB 625 and IMPRS for partial financial support. We are also grateful to Michael Kappl, Uwe Rietzler, Maren Müller, and Marcin Makowski for their help with AFS and SEM measurements and analysis.

■ REFERENCES

- (1) Alvarez, S. N.; Castano, J. L. M.; Ordieres, J. M. A.; Blanco, T. B. P. *Trends Anal. Chem.* **2008**, *27*, 437–446.
- (2) Tombelli, S.; Minunni, A.; Mascini, A. *Biosens. Bioelectron.* **2005**, *20*, 2424–2434.
- (3) Tuerk, C.; Gold, L. *Science* **1990**, *249*, 505–510.
- (4) You, K. M.; Lee, S. H.; Im, A.; Lee, S. B. *Biotechnol. Bioprocess Eng.* **2003**, *8*, 64–75.
- (5) Famulok, M.; Mayer, G.; Blind, M. N. *Acc. Chem. Res.* **2000**, *33*, 591–599.
- (6) Jenison, R. D.; Gill, S. C.; Pardi, A.; Polisky, B. *Science* **1994**, *263*, 1425–1429.
- (7) Niazi, J. H.; Lee, S. J.; Kim, Y. S.; Gu, M. B. *Bioorg. Med. Chem.* **2008**, *16*, 1254–1261.
- (8) Kota, V. K. B.; Sumedha, S. *Phys. Rev. E* **1999**, *60*, 3405–3408.
- (9) Fang, L.; Lü, Z.; Wei, H.; Wang, E. *Anal. Chim. Acta* **2008**, *628*, 80–86.
- (10) Zayats, M.; Huang, Y.; Gill, R.; Ma, C. A.; Willner, I. *J. Am. Chem. Soc.* **2006**, *128*, 13666–13667.
- (11) Baker, B. R.; Lai, R. Y.; Wood, M. S.; Doctor, E. H.; Heeger, A. J.; Plaxco, K. W. *J. Am. Chem. Soc.* **2006**, *128*, 3138–3139.
- (12) Brody, E. N.; Gold, L. *Rev. Mol. Biotechnol.* **2000**, *74*, 5–13.
- (13) Farokhzad, O. C.; Cheng, J. J.; Teply, B. A.; Sherifi, L.; Jon, S.; Kantoff, P. W.; Richie, J. P.; Langer, R. *Proc. Natl. Acad. Sci. U.S.A.* **2006**, *103*, 6315–6320.
- (14) Kim, M.; Cao, Z.; Tan, W. *Proc. Natl. Acad. Sci. U.S.A.* **2008**, *105*, 5664–5669.
- (15) Bagalkot, V.; Farokhzad, O. C.; Langer, R.; Jon, S. Y. *Angew. Chem., Int. Ed.* **2006**, *45*, 1–5.
- (16) Ruta, J.; Ravelet, C.; Grosset, C.; Fize, J.; Ravel, A.; Villet, A.; Peyrin, E. *Anal. Chem.* **2006**, *78*, 3032–3039.
- (17) Morfill, J.; Kuhner, F.; Blank, K.; Lugmaier, R. A.; Sedlmair, J.; Gaub, H. E. *Biophys. J.* **2007**, *93*, 3159–3164.
- (18) Ho, D.; Falter, K.; Severin, P.; Gaub, H. E. *Anal. Chem.* **2009**, *81*, 2400–2409.
- (19) Lee, G. U.; Chrisey, L. A.; Colton, R. J. *Science* **1994**, *266*, 771–773.
- (20) Ling, L. S.; Butt, H.-J.; Berger, R. *Appl. Phys. Lett.* **2006**, *89*, No. 113902.
- (21) Ling, L. S.; Butt, H.-J.; Berger, R. *J. Am. Chem. Soc.* **2004**, *126*, 13992–13997.
- (22) Gaub, B. M.; Kaul, C.; Zimmermann, J. L.; Carell, T.; Gaub, H. E. *Nanotechnology* **2009**, *20*, No. 434002.
- (23) Papamichael, I. K.; Kreuzer, P. M.; Guilbault, G. G. *Sens. Actuators, B* **2007**, *121*, 178–186.
- (24) Zlatanova, J.; Lindsay, M. S.; Leuba, H. S. *Prog. Biophys. Mol. Biol.* **2000**, *74*, 37–61.
- (25) Ogino, C.; Miyachi, Y.; Hayase, T.; Nosaka, K.; Kondo, A. *Ippt'6: Progress on Post-Genome Technologies, Proceedings* **2009**, *8*, 2–8.
- (26) Yu, J. P.; Jiang, Y. X.; Ma, X. Y.; Lin, Y.; Fang, X. H. *Chem.—Asian J.* **2007**, *2*, 284–289.
- (27) Jiang, Y.; Zhu, C.; Ling, L.; Wan, L.; Fang, X.; Bai, C. *Anal. Chem.* **2003**, *75*, 2112–2116.
- (28) Liu, J.; Lu, Y. *Angew. Chem., Int. Ed.* **2006**, *45*, 90–94.
- (29) Nonin-Lecomte, S.; Lin, H. C.; Patel, J. D. *Biophys. J.* **2001**, *81*, 3422–3431.
- (30) Huizenga, D. E.; Szostak, J. W. *Biochemistry* **1995**, *34*, 656–665.
- (31) Lin, C. H.; Patel, D. J. *Chem. Biol.* **1997**, *4*, 817–832.
- (32) Strunz, T.; Oroszlan, K.; Schafer, R.; Guntherodt, H. J. *Proc. Natl. Acad. Sci. U.S.A.* **1999**, *96*, 11277–11282.
- (33) Nguyen, T. H.; Lee, S. M.; Na, K.; Yang, S.; Kim, J.; Yoon, E. S. *Nanotechnology* **2010**, *21*, No. 075101.